ARTIFICIAL MAGNETIC BACTERIA:

LIVING MAGNETS AT ROOM TEMPERATURE

Magnetic nanoassemblies possess in most cases more efficient properties than magnetically-independent nanoparticles, due to their increased magnetic properties and stronger magnetic responses. As an example, the use of magnetic nanoassemblies instead of single nanoparticles can short the handling time of hyperthermia treatment because magnetic interactions can enhance their heating power[1,2].

Consequently, gaining control on the assembly of magnetic nanoparticles is a milestone that scientist should aim at. Interestingly, nature has provided an outstanding model to follow: biogenic magnetite of magnetic bacteria [3-6]. These organisms efficiently assemble single magnetic nanocrystals which are utilizd to passively align the bacteria with the geomagnetic field for orientation and navigation. Biogenic magnetite exhibits fascinating magnetic properties that could be suitable for biotechnological[7-10] however they are recalcitrant to large-scale production and they are unprecedented in their use for human oral administration. An alternative for the assembly of magnetic nanomaterials might be to replicate natural magnetic bacteria. Towards this end, efforts have been made to create structurally-mimetic magnetic bacteria by synthesizing magnetosomes in cells, either directed by the magA gene or by transfecting cells to express the magA protein[11,12]. We report a different approach. Whilst our focus was inspired by magnetotactic bacteria, we attempted to mimic their functionality rather than their structure. We used the non-magnetic probiotic bacteria *Lactobacillus fermentum* or *Lactobacillus fermentum* and *Bifidobacteria breve* as bioplatforms to densely arrange maghemite nanoparticles on their external surfaces, thus obtaining what we call artificial magnetic bacteria. These probiotic bacteria, in contrast to native magnetic bacteria, are well known to have a positive effect on the maintenance of human health since they constitute an important part of natural microbiota.

In the artificial magnetic bacteria, dipole–dipole interactions occur between nanoparticles due to their close proximity, so that maghemite nanoparticles spontaneously assemble with the application of an external magnetic field and induce the probiotic bacteria to behave as magnets at room temperature. The use of an external magnetic fi eld is in fact one of the most common routes to achieve ordered magnetic structures[13–17]. However, the ordered nanostructures thus

obtained are often limited to short-range chains which are usually prone to uncontrolled aggregation, with subsequent negative effects, for instance for biomedical applications. Our system of artificial magnetic bacteria overcomes these limitations: the presence of the bacteria as a platform facilitates the fixation of chains and the whole magnetic system remains in solution.

Results and Discussion

Our strategy to graft maghemite nanoparticles on Gram positive probiotics involves a two-step procedure in which, after halting the proliferation of probiotic bacteria, nude maghemite nanoparticles are deposited onto the bacteria biofi lm. The adsorption of magnetic nanoparticles takes place within the biofi lm, which is an extra-bacterial conglomeration of products, composed mainly of polysaccharides, that surrounds the bacterial wall. In fact, when the bacterial biofi lm was removed following a standard protocol, no assembly of particles surrounding the probiotic bacteria was observed, but a random aggregation at the extra-bacterial space was found (Figure S1). Moreover, as the biofilms are polyanionic due to the presence of either uronic acids or ketal-linked pyruvates, the nude particles are required to be positively charged[18,19] Thus, while positive maghemite nanoparticles attach onto the external bacteria surface, the negative ones show no affinity for deposition (Figure S2). We have succeeded in the preparation of a batch of artificial magnetic bacteria with iron contents ranging from 0.1 to 25 mg of iron per gram of bacteria by controlling the ratio of the amount of attached maghemite nanoparticles in regards to the quantity of bacteria. Figure 1 shows typical transmission electron microscopy (TEM) images of samples containing these two extremes of iron content.
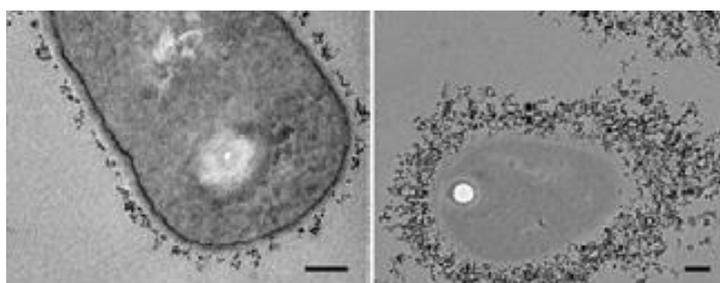
Figure 1. Typical TEM micrographs of thin epoxy resin sections of *Lactobacillus fermentum* loaded with different iron amounts. Iron contents per g of bacteria were 0.1 (left) and 25 mg (right). Scale bars are 200 nm.

The bacteria, labeled with maghemite nanoparticles, are easily redispersed in water forming a red-dark solution. The sample with the highest iron loading (25 mg of iron/g bacteria) was deeply examined, both by TEM and magnetic measurements. Large accumulations of nanoparticles were seen on the external bacterial surface in a "plum pudding" formation, where the magnetic nanoparticles are positively-charged "plums" onto a "pudding" constituted by the bacterial biofilm (Figure 2). Figure 2 b shows a typical high-resolution (HR)-TEM image of an agglomerate of nanoparticles surrounding the bacteria wall. They were well-defined, showing spherical-like topologies with heterogeneous size (average size of 10.0 nm, σ = 1.2 after measuring 100 nanoparticles). The corresponding electron diffraction pattern (Figure 2d) and measured d-spacing (Figure 2 e) were indexed according to the maghemite structure[20] X-ray powder diffraction (XRD) measurements of the magnetic colloid (Figure S3) also showed typical patterns for maghemite. Based on the calculations with the Debye–Scherrer's formula the mean maghemite nanoparticle size was 10.7 nm, accordingly with the sizes measured by TEM.
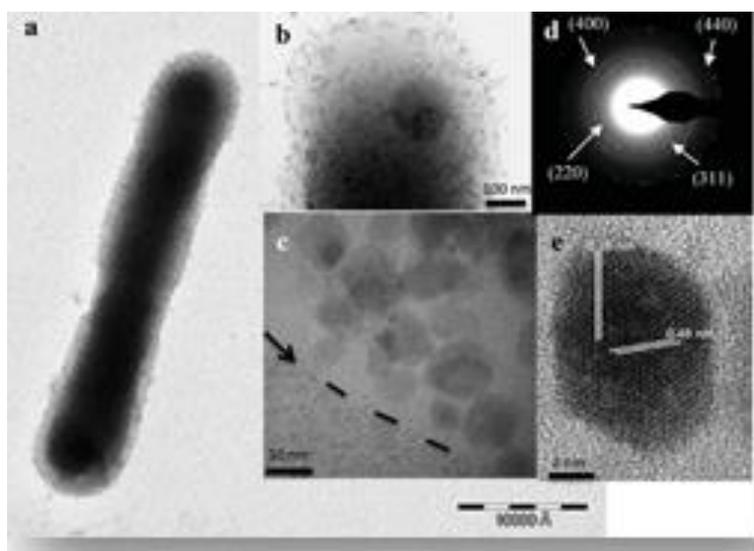

Figure 2. a) A non-contrasted TEM image of the sample containing 25 mg of iron/g of bacteria. It is noticeable that the bacterium is perfectly visible without the use of contrast, with the electron-dense maghemite nanoparticles themselves providing contrast. b) A zone at higher magnification shows the "plum pudding" structure. c) A typical HRTEM micrograph of maghemite nanoparticles

surrounding the bacterial wall (marked with an arrow in the fi gure). d) An electronic diffraction pattern of a representative particle. e) HRTEM image of a single maghemite particle with labeled d-spacing values.

The wide shell of particles surrounding the bacteria wall was visualized using high annular dark field-scanning transmission electron microscopy (HAADF-STEM; Figure 3a). To confirm the presence of the iron nanoparticles around the bacteria, energy dispersive X-ray spectroscopy (EDX) experiments were performed, which showed the juxtaposition of iron (in red) and the bacterial matrix. The spatial distribution of iron (Figure 3b), which was barely detectable inside the bacteria or in the inter-bacterial region, indicates clearly that the iron nanoparticles were incorporated into the external bacterial region, embedded in the biofi lm.
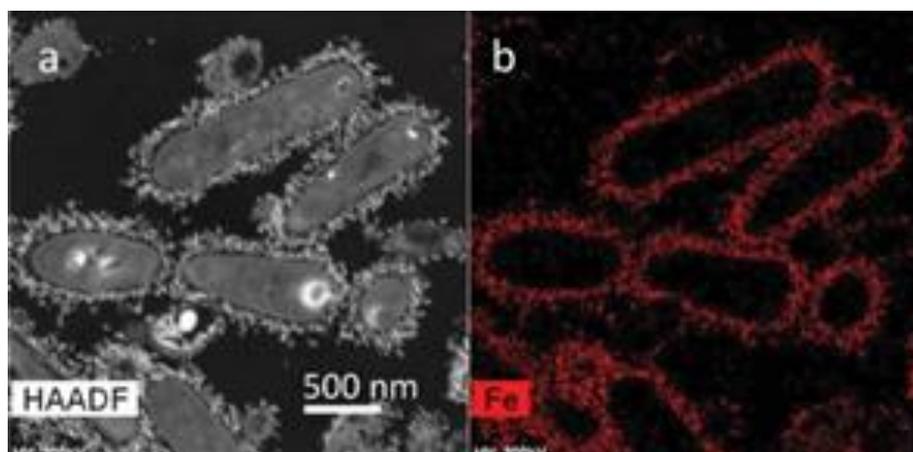

Figure 3. a) HAADF-STEM micrograph of a thin epoxy resin section showing the presence of particles at the external surface or artificial magnetic bacteria. b) EDX compositional maps of iron collected over the whole HAADF-STEM image in (a).

While individual maghemite nanoparticles of this size range (10 nm) are superparamagnetic at room temperature and do not show persistent magnetization[21,22] , the artificial magnetic bacteria of highest iron content (25 mg of iron/g of bacteria) become magnets at room temperature. This was seen without any assistance of a microscope (Figure 4). This magnetic behavior is due to the assembly process of nano particles caused by magnetic dipole–dipole interaction between them onto single bacteria. In fact, the blocking temperature (TB) of these maghemite nanoparticles shifts from 160 K to practically room temperature for the assembly of particles occurring at the artificial magnetic

bacteria with the highest iron content (Figure 4e,f). It should be noted that the broadening of the TB peak of the artificial magnetic bacteria is due to the existence of magnetic assemblies of different length and shapes, which make difficult the exact determination of TB, which can be estimated close to room temperature (Figure 4 e). Therefore, whereas the transition from the superparamagnetic to the ferromagnetic phase occurs at 160 K[22] in the maghemite nanoparticles (10 nm), this transition moves to room temperature once they are assembled onto the probiotic bacteria. It means more than 100 K higher. In fact, magnetization data at 300 K showed hysteresis with coercivity of 50 Oe (Figure 4 f), although the assemblies do not show a single-domain behavior (Mrs/Ms < 0.5) as typically found in magnetotactic bacteria.
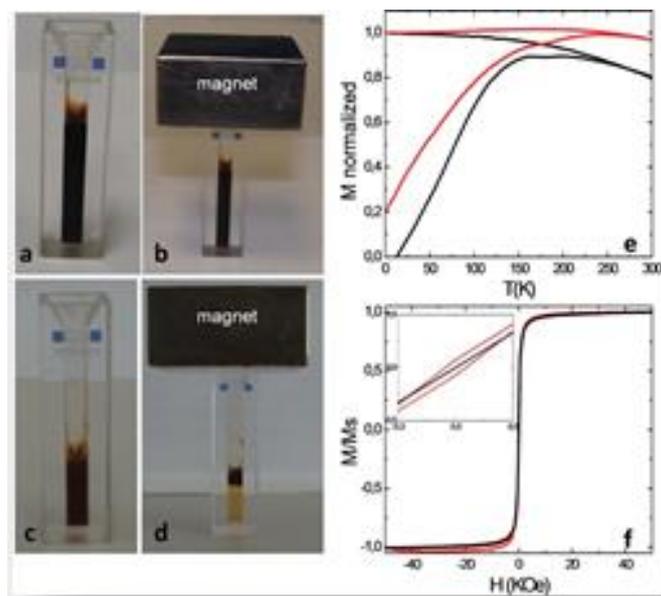

Figure 4. a) Dispersion of maghemite nanoparticles (average size of 10 nm) in aqueous media. b) The application of a magnet to the dispersion produces no effect. c) Dispersion of the highest iron-containing artifi cial magnetic bacteria in aqueous media. d) Separation of the artifi cial magnetic bacteria by application of a magnet. e) Field-cooled (FC) and zero-fi eld-cooled (ZFC) curves of lyophilized powders of maghemite nanoparticles (black) and artificial magnetic bacteria (red). f) Hysteresis curves at 300 K of lyophilized powders of maghemita nanoparticles (black) and artificial magnetic bacteria (Red). Inset: zooming of the region at low magnetic fields.

Therefore, the artificial magnetic bacteria behave as magnets at room temperature, mimicking the key feature of natural magnetotactic bacteria, despite their

structures bear no similarity. While natural magnetic bacteria usually contain internal chains of a few magnetic nanocrystals, our artificial magnetic bacteria are enriched with thousands of magnetic nanoparticles deposited at their external surface.

The artificial magnetic bacteria showed the ability to swim (Figure S4) and be guided towards a target when exposed to a directional magnetic fi eld. The artificial magnetic bacteria were labeled with fluorescent green SYTO9 (Figure 5) to visualize the response to an external magnetic field. This fluorophore is commonly used for the labeling of live bacteria, which, incidentally, demonstrated that the bacteria remain alive after grafting the magnetic nanoparticles. As it is shown in Figure 5, on placing a permanent magnet (0.3 T) to a drop of aqueous solution of the artificial magnetic bacteria deposited in polylysine glass, magnetic nanoassembly occurred. The artificial magnetic bacteria became directionally arranged following the magnetic fi eld lines. Note that the application of the same external magnet to the maghemite nanoparticles in the absence of bacteria produces no effect (Figure 3 b). This fact points out the crucial role of the bacteria as platforms to assembly the magnetic nanoparticles and therefore inducing the artificial bacteria to behave as magnets at room temperature. The similarities and differences between the biogenic and our biometic magnetic bacteria should be highlighted here. Firstly, nature chose magnetite crystals of the appropriate size, usually larger than 50 nm[3,4] .This is a wise "decision" of nature, since smaller crystals would not contribute efficiently to the bacteria magnetic moment. However, here we demonstrate that we can produce, from superparamagnetic small maghemite nanoparticles (10 nm in size), magnetic bacteria that present a collective ferromagnetic phase at room temperature, although a single domain behavior was not reached.
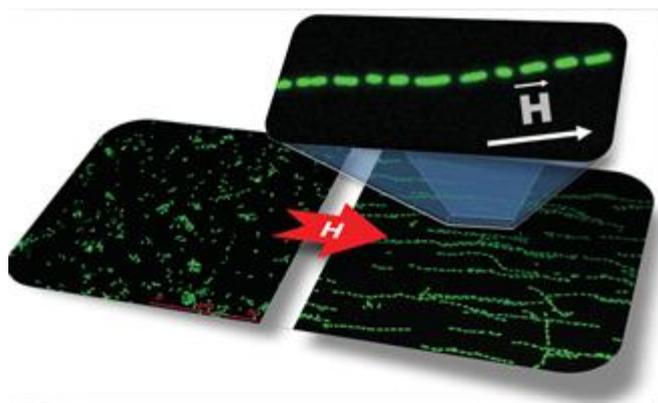
Figure 5. Arrangement on polylysine glass of the artificial magnetic bacteria labeled with the green SYTO9 after applying an external magnetic field. Inset: A single chain fragment is magnified to highlight the magnetic order of these artificial magnetic bacteria. Every fluorescent spot corresponds to an artificial magnetic bacterium.

On the other hand, in our biomimetic magnetic bacteria, a 3D cylindrical shell architecture is built from maghemite nanoparticles that implies a highly complex process of assembly. Interestingly, this assembly (Figure 4) resembles the filamentous structure of twisted strands found in some magnetotactic bacteria, [23] with the difference that while in our artificial magnetic bacteria every brick is by itself a magnetic bacterium, in biogenic magnetic bacteria, the bricks are magnetosomes. From a crude magnetic point of view, artificial magnetic bacteria differ from most native ones. Thus, whereas some native magnetic bacteria are able to align themselves with the Earth magnetic field (50 µT), the minimal magnetic fi eld required for arranging the artificial bacteria was 30 mT. However, it should be noted that, the functional magnetosome chains usually aggregate when extracted from native bacteria. This aggregation worsens their magnetic properties and therefore their biomedical applications. In fact, a decrease in the coercivity and reduced remanence is observed in extracted magnetosomes if compared with the whole magnetotactic bacteria [24]. Nevertheless, and in order to advance in the pursuit of mimicking their functionality as closely as possible, we wanted to take advantage of their features. The artificial magnetic bacteria resulted to exhibit some magnetic behaviors that reminded those of the native ones: the possibility to be magnetically ordered (Figure 5) and the ability to swim in an aqueous solution when an external magnetic field was applied (Figure S4).

But, at the same time, our synthetic system presented some advantages with respect to the native one. Firstly, it provided fl exibility for monitoring the iron loading per bacterium.

Interestingly, in all the assayed iron content range, most bacteria remain alive and in fact, the viability does not fall below $1 \cdot 10^8$ CFU (colony forming units), which is in the range of the accepted values for labeling bacteria as a probiotic (see Experimental Section). Secondly, the probiotic are not unprecedented in human administration since their well-known healthy effect, in particular in the promotion of the immune system activity, the defense against infections and because their anti-infl ammatory properties[25,26].

Furthermore, certain probiotics have emerged as biological vectors with tumor specificity and therapy activity[27] as due to their anaerobic nature of probiotic, they are known to specifically localize at the hypoxic regions of solid tumors [28,29].

Conclusion

We have developed a simple and powerful methodology to create magnetic bacteria from superparamagnetic nanoparticles and probiotics. The artificial magnetic bacteria resulted to exhibit some magnetic behaviors that reminded the key features of native ones: they are alive and become magnetically ordered at room temperature, although the magnetic fi eld required is sensible higher than the geomagnetic one. However, this synthetic system presented some advantages with respect to the native one: flexibility for monitoring the iron loading per bacterium and good viability.

In the basis on their magnetic properties, these artificial magnetic bacteria, as it occurs for native ones, have a broad window of biomedical applications, i.e., MRI, hyperthermia, biosensors, etc.[7–10]. However, it must be emphasized that while native magnetic bacteria are unprecedented in their administration to humans, our artifi cial magnetic bacteria are made of probiotic bacteria, widely incorporated in food since they confer health benefi ts for humankind. In addition, our procedure involves mild chemical conditions and may be easily adapted to large-scale production. All these aspects provide additional value to this research[30].

References

1. M. Vallet-Regi , E. Ruiz-Hernández, 2011 , *23* , 5177 .
2. B. Mehdaoui , R. P. Tan, A. Meffre, J. Carrey, S. Lachaize, B. Chaudret , M. Respaud , *Phys. Rev. B: Cond. Matt. and Mater. Phys.* 201, *87*, 174419/1.
3. Schüler, *FEMS Microbiol. Rev.* 2008, 32, 654.
4. A. Bazylinski, R. B. Frankel, *Nat. Rev. Microbiol.*2004 , *2* , 217 .
5. a) Z. Tang , N. A. Kotov , *Adv. Mater.* 2005, *17*, 951; b) E. Bäuerlein , *Angew. Chem. Int. Ed.* 2003, *42*, 614.
6. D. Schüler, *Microbiology Monographs* Vol. *3* , Springer , Heidelberg 2006 .
7. D. Schüler, R. B. Frankel, Appl*. Microbiol. Biotechnol.* 1999, 52, 464 .
8. E. Alphandéry, S. Faure, O. Seksek, F. Guyot , I. Chebbi, *ACS Nano* 2011 , *5* , 6279 .
9. C. Lang, D. Schüler, D. Faivre, *Macromol. Biosci.* 2007, *7*, 144 .
10. T. Matsunaga, T. Suzuki, M. Tanaka, A. Arakaki, *Trends Biotechnol.* 2007, 25, 182.
11. X. P. Hu, A. W.-S. Chan, O. Zurkiya, Patent WO 2006119102 A1 20061109, 2006 .
12. K. Nishida, P. A. Silver, *PLoS Biol.* 2012, *10*, e1001269 .
13. Z. H. Nie, A. Petukhova, E. Kumacheva , *Nat. Nanotechnol.* 2010 ,*5* ,15 .
14. Y. Min, M. Akbulut , K. Kristiansen , Y. Golan , J. Israelachvili , *Nat. Materials* 2008 , *7* , 527.
15. Y. Lu, L. Dong, L.-C. Zhang, Y.-D. Su, S.-H. Yu, *Nano Today* 2012, *7*,297.
16. M. D. Krebs, R. M. Erb, B. B. Yellen, B. Samanta, A. Bajaj, V. M. Rotello, E. Alsberg, *Nano Lett.*2009, *9*, 1812 .
17. N. Leventis, I. A. Elder, J. L. Gary, D. R. Rolison, *Nano Lett.* 2002, *2*, 63.
18. S. C. Hayden, G. Zhao, K. Saha, R. L. Phillips, X. Li, O. Miranda, V. M. Rotello, M. A. El-Sayed, I. Schmidt-Krey, U. H. F. Bunz , *J. Am. Chem. Soc.* 2012, *134*, 6920 .
19. V. Berry, R. F. Saraf, *Angew. Chem. Int. Ed.* 2005, *117*, 6826 .
20. T. Hyeon, S. S. Lee, J. Park, Y. Chung, H. B. Na, *J. Am. Chem. Soc* 2001, *123*, 12798.
21. Valero, S. Tambalo, P. Marzola, M. Ortega-Muñoz, J. Lopez-Jaramillo, F. Santoyo, J. D. Lopez, J. J. Delgado, J. J. Calvino, R. Cuesta, J. M. Domínguez-Vera, J. M., Santoyo-Gónzalez, N. Gálvez, *J. Am. Chem. Soc.* 2011, *133*, 4889.
22. J. Park , E. Lee, N. M. Hwang, M. Kang, S. C. Kim, Y. Hwang, J.-G. Park, H.-J. Noh, J.-Y. Kim, J.-H. Park, T. Hyeon, *Angew. Chem. Int. Ed.* 2005, *44*, 2872.
23. D. Schüler, *Biomineralization* (Ed: E. Baeuerlein), Wiley-VCH, Weinheim 2000 p.109.
24. E. Alphandéry, A. T. Ngo, C. Lefèvre , I. Lisiecki , L. F. Wu , M. P. Pileni , *J. Phys. Chem.* 2008 , *112* , 1 2304 .
25. M. E. Sanders, F. Guarner, R. Guerrant, P. R. Holt, E. M. M. Quigley, R. B. Sartor, P. M. Sherman, E. A. Mayer, *Gut* 2013, 62, 787.
26. Lara-Villoslada, M. Olivares, S. Sierra, J. M. Rodríguez , J. Boza, J. Xaus, *British J. Nutrition* 2007, *98*, S96 .
27. M. Cronin, D. Morrissey, S. Rajendran, S. M. El Mashad, D. van Sinderen, G. C. O'Sullivan, M. Tangney, *Mol. Therapy* 2010, *18*, 1397.
28. X. Li, G. F. Fu, Y. R. Fan, W. H. Liu, X. J. Liu, J. J. Wang, X. Gen-Xing, *Cancer Gene Ther.* 2003, 10, 105.
29. T. Nakamura, T. Sasaki, M. Fujimori, K. Yazawa, Y. Kano, J. Amano, S. Taniguchi, *Biosci. Biotechnol. Biochem.* 2002, *66*, 2362.
30. J. M. Domínguez-Vera, N. Gálvez, M. Martín, F. Carmona, D. Rondón, M. Olivares, (Biosearch SA) Patent Cooperation Treaty (PCT), P8748EP00, 2013.